UC Irvine
UC Irvine Previously Published Works

Title

Adult MTM1-related myopathy carriers: Classification based on deep phenotyping.

Permalink

https://escholarship.org/uc/item/7dt1z7t5

Journal

Neurology, 93(16)

ISSN

0028-3878

Authors

Cocanougher, Benjamin T
Flynn, Lauren
Yun, Pomi
et al.

Publication Date

2019-10-15

DOI

10.1212/wnl.0000000000008316

Peer reviewed

Adult *MTM1*-related myopathy carriers

Classification based on deep phenotyping

Benjamin T. Cocanougher, BS, Lauren Flynn, DO,* Pomi Yun, MPH,* Minal Jain, DSc, PT, Melissa Waite, MSPT, Ruhi Vasavada, BS, Jason D. Wittenbach, PhD, Sabine de Chastonay, PhD, Sameer Chhibber, MD, A. Micheil Innes, MD, Linda MacLaren, MS, CGC, Tahseen Mozaffar, MD, Andrew E. Arai, MD, Sandra Donkervoort, MS, CGC, Carsten G. Bönnemann, MD, and A. Reghan Foley, MD

Correspondence
Dr. Foley
reghan.foley@nih.gov

Abstract

Objective
To better characterize adult myotubularin 1 (*MTM1*)–related myopathy carriers and recommend a phenotypic classification.

Methods
This cohort study was performed at the NIH Clinical Center. Participants were required to carry a confirmed *MTM1* mutation and were recruited via the Congenital Muscle Disease International Registry (n = 8), a traveling local clinic of the Neuromuscular and Neurogenetic Disorders of Childhood Section, National Institute of Neurological Disorders and Stroke, NIH and Cure CMD (n = 1), and direct physician referral (n = 1). Neuromuscular examinations, muscle MRI, dynamic breathing MRI, cardiac MRI, pulmonary function tests (PFTs), physical therapy assessments including the Motor Function Measure 32 (MFM-32) scale, and X chromosome inactivation (XCI) studies were performed.

Results
Phenotypic categories were proposed based on ambulatory status and muscle weakness. Carriers were categorized as severe (nonambulatory; n = 1), moderate (minimal independent ambulation/assisted ambulation; n = 3), mild (independent ambulation but with evidence of muscle weakness; n = 4), and nonmanifesting (no evidence of muscle weakness; n = 2). Carriers with more severe muscle weakness exhibited greater degrees of respiratory insufficiency and abnormal signal on muscle imaging. Skeletal asymmetries were evident in both manifesting and nonmanifesting carriers. Skewed XCI did not explain phenotypic severity.

Conclusion
This work illustrates the phenotypic range of *MTM1*-related myopathy carriers in adulthood and recommends a phenotypic classification. This classification, defined by ambulatory status and muscle weakness, is supported by muscle MRI, PFT, and MFM-32 scale composite score findings, which may serve as markers of disease progression and outcome measures in future gene therapy or other clinical trials.

---

*These authors contributed equally to this work.

From the University of Rochester School of Medicine and Dentistry (B.T.C.), NY; Howard Hughes Medical Institute Janelia Research Campus (B.T.C., J.D.W.), Ashburn, VA; St Catharine's College (B.T.C.), University of Cambridge, UK; Clinical Center, NINDS (L.F.), Neuromuscular and Neurogenetic Disorders of Childhood Section, Neurogenetics Branch, NINDS (P.Y., S.D.C., C.G.B., A.R.F.), Clinical Research Center, Rehabilitation Medicine Department (M.J., M.W., R.V.), and Advanced Cardiovascular Imaging Laboratory, NHLBI (A.E.A.), NIH, Bethesda, MD; Congenital Muscle Disease International Registry (CMDIR) (S.d.C.), Cure CMD, Torrance, CA; Department of Medical Genetics and Alberta Children's Hospital Research Institute, Cumming School of Medicine (A.M.I.), and Department of Clinical Neurosciences (S.C.), University of Calgary; Department of Medical Genetics and Alberta Children's Hospital (L.M.), Calgary, Canada; and Department of Neurology (T.M.), University of California, Irvine.

Go to Neurology.org/N for full disclosures. Funding information and disclosures deemed relevant by the authors, if any, are provided at the end of the article.

Glossary

FVC = forced vital capacity; **MFM-32** = Motor Function Measure 32; ***MTM1*** = myotubularin 1; **PFT** = pulmonary function test; **SID** = SET-interacting domain; **XCI** = X chromosome inactivation.

Myotubularin 1 (*MTM1*)–related myopathy (OMIM 310400), also called myotubular myopathy or X-linked myotubular myopathy, leads to severe weakness in male infants.[1] In the absence of supportive care, most affected males die during infancy of respiratory insufficiency. Disease manifestations in adult female carriers occur; however, they have not been systematically investigated. In total, 57 cases of manifesting and nonmanifesting carriers of *MTM1*-related myopathy have been described in 17 reports, exhibiting a spectrum of disease from manifesting predominantly with limb-girdle weakness to severe, generalized congenital weakness (table e-1, doi.org/10.5061/dryad.116n37m).[2–18] Left–right asymmetry of weakness and skeletal size has been observed in a few reports.[5,10,11,18] Here we report 10 previously unreported carriers of *MTM1*-related myopathy who were deeply phenotyped under a standardized protocol at the NIH by muscle MRI, dynamic breathing MRI, cardiac MRI, pulmonary function tests (PFTs), the Motor Function Measure 32 (MFM-32) scale,[19] and X chromosome inactivation (XCI) studies. We develop disease severity categories and present clinical findings that should raise a clinician's suspicion for *MTM1*-related myopathy. A gene therapy trial for male infants with *MTM1*-related myopathy is currently in progress, which provides hope for a potential therapeutic intervention for *MTM1*-related myopathy carriers.

Methods

Patients and data

Ten genetically confirmed *MTM1*-related myopathy carriers were recruited through the Congenital Muscle Disease International Registry (n = 8), via a traveling local clinic arranged by the Neuromuscular and Neurogenetic Disorders of Childhood Section, National Institute of Neurological Disorders and Stroke, NIH and Cure CMD (n = 1); and by direct physician referral (n = 1). History and full neuromuscular examinations, muscle MRI, dynamic breathing MRI, cardiac MRI, pulmonary function tests, and physical therapy assessments including the MFM-32 scale[19] were performed at the NIH Clinical Center.

Standard protocol approvals, registrations, and patient consents

Approval from the institutional review board of the NIH was received, and all participants were enrolled with written informed consent under protocol 12-N-0095 at the NIH.

Weakness visualization

Custom open-source software named MuscleViz[20] was developed for displaying muscle weakness findings. Plots can be generated using a free online browser application or as a free mobile application for Apple iOS or Android devices.

XCI studies

XCI studies were performed on peripheral blood samples as previously described.[21] A ratio of less than 80:20 is considered random, between 80:20 and 90:10 is moderately skewed, and greater than or equal to 90:10 is highly skewed.

Imaging

Chest wall, diaphragm, and cardiac MRI was performed on a 3T (n = 7) or 1.5T scanner (n = 2). Chest wall and diaphragm imaging was done with real-time cine MRI (dynamic breathing MRI) for 10–20 seconds with a typical temporal resolution of about 41 ms. Cardiac MRI included cine MRI of cardiac volumes and function, native myocardial T1, native myocardial T2, and late gadolinium enhancement imaging. Muscle MRI was performed on a 3T scanner and included T1 axial imaging of the lower extremities.

Data availability

Anonymized data will be shared by request with any qualified investigator.

Results

MTM1-related myopathy carriers were between 27 and 64 years old at the time of evaluation. Carriers exhibited a range of symptom severity, from severe muscle weakness with loss of ambulation by the third decade (M1) to no muscle weakness but with evidence of skeletal asymmetry (M10) (figure 1, table 1). The pattern of muscle weakness was predominantly proximal and limb-girdle in distribution, as seen in 8 of the 10 carriers (M1–M8) (figure 1B). Of these 8 carriers, all but M6 had asymmetric muscle weakness and asymmetric skeletal size with evidence of a smaller hand on the side of greater muscle weakness. Distal muscle weakness was also present in patients categorized as severe (M1) and moderate (M2–M4) (figure 1B). The MFM-32 composite score captured motor phenotypic severity in 3 domains, and the resulting scores parallel our prespecified phenotypic classification of carriers as severe (nonambulatory): M1; moderate (minimal independent ambulation/assisted ambulation): M2–M4; mild (independent ambulation but with evidence of muscle weakness): M5–M8; and nonmanifesting (no evidence of muscle weakness): M9–M10 (figure e-1, doi.org/10.5061/dryad.116n37m).

Eight of the 10 *MTM1*-related myopathy carriers exhibited clinically recognizable skeletal asymmetries, most notably

Figure 1 Clinical phenotype, muscle imaging findings, and muscle histotype
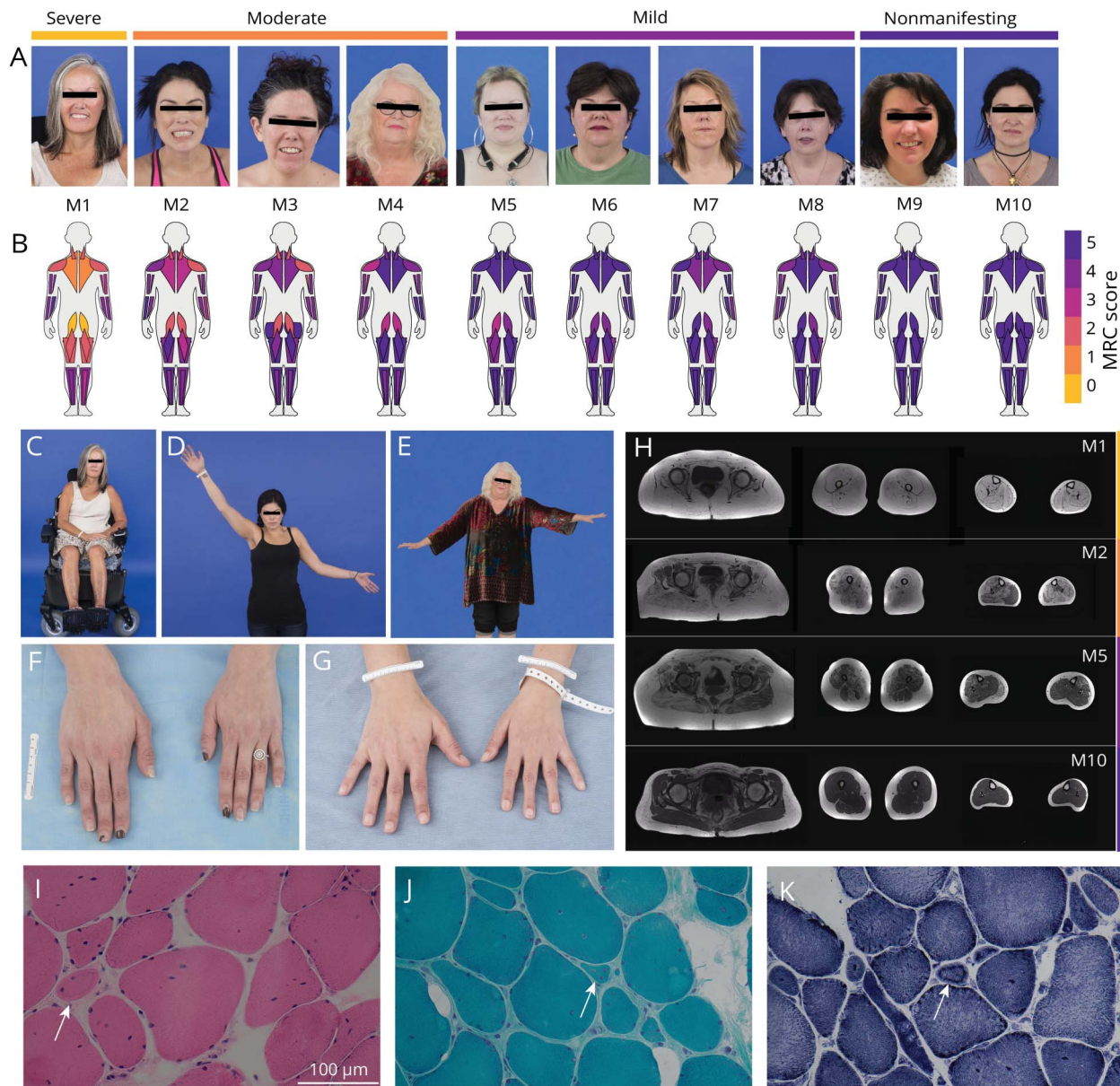
(A) We phenotypically categorized carriers as severe (nonambulant) (M1), moderate (minimal independent ambulation/assisted ambulation) (M2–M4), mild (independent ambulation but with evidence of muscle weakness) (M5–M8), and nonmanifesting (no evidence of muscle weakness) (M9 and M10). (B) MuscleViz, a custom open-source software package, was created to visualize weakness using the Medical Research Council (MRC) scale for muscle strength. Plots can be generated using a free online browser application: muscleviz.github.io/. (C) The patient phenotypically categorized as most severe (M1) was wheelchair dependent by her third decade. (D, E) Patients M2 and M4's asymmetric weakness is revealed by the inability to raise the weaker arm as high as the stronger one. (F, G) Patients M2 and M3 have evidence of asymmetric skeletal growth, presenting as a difference in hand size, both with evidence of the left hand being smaller than the right hand. (H) Muscle MRI of the lower extremities reveals abnormal T1-weighted signal in all leg muscles imaged in M1 (severe), significantly increased T1 signal in the left medial gastrocnemius muscle, and normal T1 signal in the right medial gastrocnemius muscle in M2 (moderate) with prominent left–right asymmetry of lower leg muscle sizes below the knee, increased T1 signal in the right medial gastrocnemius muscle and right semitendinosus muscle in M5 (mild), and normal-appearing signal and size of all lower extremity muscles imaged in M10 (nonmanifesting). (I–K) Right vastus lateralis biopsy performed in M3 at 32 years of age with evidence of rare, subtle necklace fibers (arrows) on hematoxylin & eosin stain (×40) (I), Gömöri trichrome stain (×40) (J), and nicotinamide adenine dinucleotide stain (×40) (K). Measurement bar = 100 μm.

facial asymmetries, manifesting as hemifacial hypoplasia (M1–M4, M8, and M10) and differences in hand size (M1–M5, M7, and M8) (figure 1). Asymmetry of facial skeletal size was evidenced by left–right asymmetry of orbital fissure size and was not always associated with the degree of muscle weakness, as seen in patient M10 (nonmanifesting).

All 10 patients underwent lower extremity muscle MRI (figure 1H). M5 had increased T1 signal in the medial gastrocnemius muscle on the right side only and selective involvement of the right semitendinosus muscle. All patients classified as moderate or mild (M2–M8) had evidence of abnormal T1 signal in specific muscles, often differing between the left and the right, with abnormal muscle signal

Table 1 Patient characteristics

	M1	M2	M3	M4	M5	M6	M7	M8	M9	M10
Phenotypic classification	Severe	Moderate	Moderate	Moderate	Mild	Mild	Mild	Mild	Nonmanifesting	Nonmanifesting
***MTM1* mutation**	c.529-2A > G	c.1356_1357delCC; p.P453Yfs*4	Deletion exons 1-15	c.1792delC; p.H598Mfs*23	c.1519_1522delGAAA; p.E507Nfs*28	c.2T > G; p.M1R	c.2T > G; p.M1R	c.1260+5 G > A	c.205C > T; p.R69C	c.205C > T; p.R69C
Mutation reference	Novel	Novel	Dahl et al., 1995[4]; Biancalana et al., 2017[18]	Herman et al., 1999[23]; Herman et al., 2002[25]	LOVD ID MTM1_00245	Herman et al., 1999[23]; Herman et al., 2002[25]	Herman et al., 1999[23]; Herman et al., 2002[25]	ClinVar RCV000146390	Pierson et al., 2012[24]	Pierson et al., 2012[24]
X chromosome inactivation ratio	66:34	78:22	79:21	52:48	59:41	100:0	69:31	98:2	66:34	73:27
Affected relatives (age at death)	None	Twin sons (14 mo)	None	1 son (4 y)	1 son (2 y)	1 son (8 y)	Twin brother (newborn)	1 son (9 y)	Twin sons (7 y); identical twin living at 9 y	1 son (15 y)
Age at examination, y	48	27	36	64	30	47	44	53	46	51
First sign/ symptom	Unable to run (5 y)	Unable to rise from the floor and difficulty running (5 y)	Difficulty running, skipping, and jumping (childhood)	Difficulty with endurance (10 y)	Repeated ankle sprains (14 y)	"Clumsy" (childhood)	No motor symptoms reported	Easy fatigability, difficulty holding arms above head and leg cramping (childhood)	Difficulty running in relay races (6 y)	Not symptomatic
Achieved running	No	No	Yes	Yes	Yes	Yes	Yes	Yes	Yes	Yes
Independent ambulation?	No (motorized wheelchair dependent)	Yes (short distances)	No (assisted with cane)	No (assisted with cane)	Yes	Yes	Yes	Yes	Yes	Yes
FVC (% predicted)	23	58	83	36	82	92	91	67	93	107
Noninvasive ventilation use (age started, y)	BiPAP (48)	BiPAP (27)	No	BiPAP (59)	No	No	No	CPAP (51)	No	No
Echocardiogram ejection fraction, %	55	NA	60	65	60	70	56	60	64	65

Abbreviations: BiPAP = bilevel positive airway pressure; CPAP = continuous positive airway pressure; FVC = forced vital capacity; NA = not available.

apparent on the clinically weaker side. Muscle MRI revealed normal-appearing signal and size of muscles in both non-manifesting carriers (M9 and M10).

Nine patients (M1–M9) underwent dynamic breathing MRI and cardiac MRI. Patient M1 had evidence of a significant pectus excavatum (Haller index of 6.5 [normal 2.56 ± 0.35] [22]). Patients M2, M6, and M8 demonstrated predominantly diaphragmatic motion with minimal chest wall motion during free breathing and clear augmentation of diaphragmatic motion with lesser augmentation of chest wall motion with deep breathing. Patients M3, M5, M7, and M9 also had predominant diaphragmatic motion with free breathing; however, they had evidence of appropriate augmentation of both diaphragmatic and chest wall motion with deep breathing. Patient M4 had left-sided hemidiaphragm elevation. She demonstrated movement of both sides of the diaphragm and equal contributions of diaphragmatic and chest wall motion with free and deep breathing. Cardiac MRI showed normal global and regional left ventricular function in all 9 patients imaged. No clinically recognized myocardial fibrosis or infarction on late gadolinium-enhanced imaging was appreciated.

Greater decreases in forced vital capacity (FVC) were seen in carriers with more severe muscle weakness (table 1). Within each phenotypic category, the oldest patient had the lowest FVC value. Nonmanifesting carriers had FVC values within the normal reference range.

XCI testing was performed (figure 2, B and C). Two patients (M6 and M8) of the mild phenotype group had highly skewed XCI patterns, while the remaining 8 patients, including patient M1 with a severe phenotype and patients M9 and M10 with a nonmanifesting phenotype, had random patterns (<80:20). There was no apparent association between the severity of asymmetry in muscle weakness and skeletal growth and the XCI pattern. The *MTM1* mutation status of the predominately active X chromosome was not assessed.

All patients are heterozygous carriers of an *MTM1* mutation (figure 2A). Two mutations in the cohort (M1 and M2) have not been reported in the literature or online databases, and 8 mutations (M3–M10) have been previously reported in male patients (table 1).[4,18,22–24] The most severely affected patient (M1) has a novel mutation in a splice acceptor site in intron 7 of *MTM1*, which is predicted to result in a truncated protein that is missing both the protein tyrosine phosphatase domain and SET-interacting domain (SID). The second novel mutation, observed in patient M2, is a frameshift mutation in the middle of the SID in exon 13.

Missense mutations resulted in a mild phenotype and were clustered in exons 2 and 4; none of these missense mutations affects the active site of the protein directly. Splice site mutations were associated with a spectrum of phenotypic severity and were found in introns 7 and 11. Frameshift mutations were associated with a moderate or mild phenotype and were found in exons 13, 14, and 15. A 515 kb deletion that

Figure 2 *MTM1* gene mutation locations and X-inactivation ratios for manifesting and nonmanifesting carriers
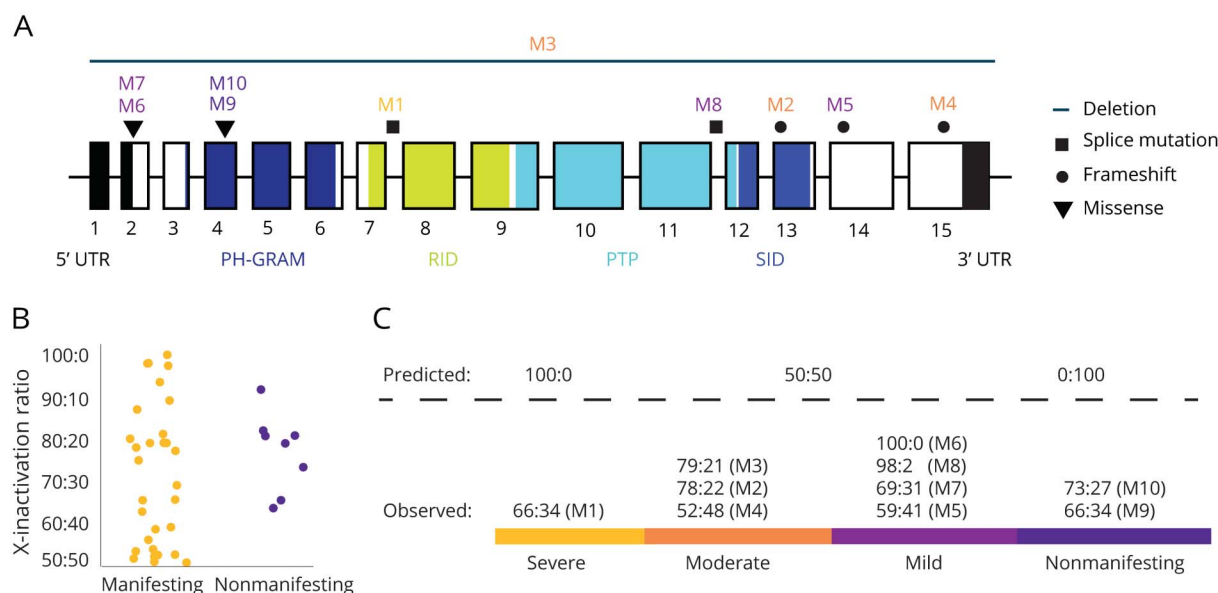
(A) Gene structure and location of mutations in the *MTM1* gene. Exons are represented as boxes. Mutation locations are indicated with mutation type coded by shape. The myotubularin protein contains 4 domains: the pleckstrin homology glucosyltransferases, Rab-like GTPase activators and myotubularins (PH-GRAM) domain, Rac1-Induced recruitment domain (RID), protein tyrosine phosphatase (PTP) and SET-interacting domain (SID). (B) X-inactivation ratios for *MTM1*-related myopathy manifesting and nonmanifesting carriers reported in the literature show a range of ratios without a clear pattern. (C) X-inactivation patterns are expected to follow predicted ratios if X-inactivation is the primary driver of symptom expression and severity; however, the prediction does not hold up in our cohort, suggesting the X-inactivation model of disease expression is incomplete, and additional factors exist.

included the entire coding region of the *MTM1* gene and surrounding genes (*MAMLD1*, *MTMR1*, and *CD99L2*) was associated with a moderate phenotype (M3). Mutations that resulted in complete loss of the protein or potential alterations in the SID were associated with more severe muscle weakness and skeletal asymmetry (M1–M3).

Patients M6 and M7 are siblings and share a previously reported missense mutation (c.2T > G) affecting the starting methionine (p.M1R) (figure 2A; Leiden ID MTM1_00007).[25,26] Patients M9 and M10 are unrelated but share a previously described missense mutation (c.205C > T) resulting in a p.R69C substitution and a skipping event in exon 4.[24]

Discussion

We phenotyped a cohort of 10 previously unreported adult *MTM1*-related myopathy carriers who we systematically assessed with a preplanned protocol. The use of dynamic breathing MRI and cardiac MRI had not been previously reported in *MTM1*-related myopathy carriers. These tools were utilized to more completely characterize these aspects of the phenotype for future clinical reference. Skeletal muscle and respiratory muscle weakness appear to be commensurate in degree and progressive in nature in carriers who develop muscle weakness by young adulthood. Notably, the MFM-32 composite scores parallel our proposed phenotypic classification. Given that *MTM1*-related myopathy carriers were recruited for this study via a patient registry as well as via clinician referral, this cohort is likely skewed towards manifesting carriers. Taken together, however, the deep phenotyping of manifesting carriers of various clinical severity in this cohort has highlighted the range of muscle weakness and respiratory insufficiency that can be observed in carriers.

Deep phenotyping of complex phenotypes, such as can be seen in *MTM1*-related myopathy carriers, can help to characterize features that may be missed by routine clinical examination and testing. We performed dynamic breathing MRI and cardiac MRI in order to screen for subtle respiratory and cardiac abnormalities. Our dynamic breathing MRI results reveal direct imaging evidence of the degree of chest wall weakness exceeding the degree of diaphragmatic weakness. Comparing FVC values in upright versus supine PFTs can more routinely evaluate the relative contribution of diaphragmatic weakness to decreased pulmonary function. Our cardiac MRI results did not uncover abnormalities in myocardial appearance or cardiac function, indicating that detailed cardiac imaging using MRI is not necessary for clinical surveillance of carriers.

Left–right asymmetries of skeletal size, as observed in female carriers of *MTM1* mutations, have been reported only once in a mildly affected male patient with *MTM1*-related myopathy.[14] It is notable that the severity of skeletal asymmetry did not consistently match the severity of muscle weakness in our cohort, as exemplified by patient M10, who has evidence of right hemifacial hypoplasia in the setting of normal skeletal muscle strength and normal muscle MRI findings. This raises the possibility of distinct pathways for myotubularin in skeletal bone growth and skeletal muscle development, which is compatible with the existence of multiple isoforms of myotubularin and tissue-specific expression.[27] Left–right asymmetries of muscle size on muscle MRI have also been noted in facioscapulohumeral muscular dystrophy,[28,29] in female carriers of dystrophinopathy,[30] in *ANO5*-related muscular dystrophy,[31] in *FHL1*-related disorders,[32] and in dysferlinopathies.[33] These muscular dystrophies manifest differences in muscle size but not skeletal size. Asymmetric skeletal growth (in addition to asymmetric muscle size) appears to be a distinguishing characteristic of *MTM1*-related myopathy carriers.

Skewed XCI has been hypothesized as a mechanism to explain symptom manifestation[5,10,11,34] and asymmetric findings[18]; however, a recent review of 24 previously reported cases of manifesting *MTM1*-related myopathy carriers found no correlation between skewed XCI and disease manifestation.[17] Our data also do not support the hypothesis of skewed XCI as a primary or sole etiology of disease manifestation (figure 2, B and C), and our review of 40 cases in the literature reveals a similar discordance between experimental results and model expectations (figure 2B and table e-1, doi.org/10.5061/dryad.116n37m). Studies in *MTM1*-related myopathy have found different ratios of XCI in patient blood vs muscle samples[9] and in blood vs cultured fibroblasts.[6] Furthermore, XCI patterns are a dynamic process that vary in a tissue-specific manner and over time as patients age,[34–36] thus age-dependent variability of XCI may indeed be a factor in the progressive nature of symptoms in carriers. In order to test the XCI model, future studies would need to consider testing the XCI ratio comparatively in the differentially affected muscles. This approach would require that muscle biopsies be performed in individual patients in both weak and full strength muscle groups, however. If XCI is playing a role in clinical severity, it would be expected that weaker muscles would have skewed XCI resulting in higher levels of the mutated X. Even if XCI is determined to be a factor in the manifestation of symptoms, additional disease modifiers remain likely. Variations in dynamin 2 (DNM2) levels, for example, have been shown in animal models to be an autosomal disease modifier, where a decreased level can ameliorate the *MTM1*-related myopathy disease severity.[37,38] Bridging integrator 1 (BIN1) or amphiphysin 2 (AMPH2) equally interplays with that balance.[39] Here we propose a third potential modifier: escape from XCI. Recent reports reveal that at least 23% of human genes consistently escape XCI.[40–42] The amount of escape varies within an individual (in a tissue-specific manner) and between individuals.[43] The *MTM1* gene is subject to escape from XCI and was reported to escape XCI in 11% of women.[44] An increase in escape from XCI of a deleterious copy or a lack of escape by a functional copy of *MTM1* may play a role in variable symptom manifestation.

Establishing a diagnosis of *MTM1*-related myopathy in carriers without a family history of the disease can be challenging. Asymmetric muscle weakness and asymmetric skeletal size were important diagnostic clues for patients M1 and M3, in whom there was no history of an affected offspring or an affected sibling. Both M1 and M3 had undergone 2 nondiagnostic muscle biopsies. The histologic finding of necklace fibers is highly suggestive but not pathognomonic for *MTM1*-related myopathy.[14,18,44] Necklace fibers were noted in M3's third muscle biopsy (figure 1, I–K) during a re-review of this biopsy due to clinical suspicion of *MTM1*-related myopathy.

A promising gene therapy trial for male patients with *MTM1*-related myopathy is in progress (ClinicalTrials.gov Identifier: NCT03199469). The outcome of this trial will determine whether this gene therapy may be extended to female manifesting carriers. Thus, gene therapy carries promise not only for affected male patients but also for female manifesting carriers of *MTM1*-related myopathy. Muscle MRI, PFTs, and the composite score of the MFM-32 scale confirm our prespecified phenotypic classification, which, along with the clinical assessments of motor and pulmonary function, may be used as biomarkers of disease progression and may qualify as outcome measures in future clinical trials.

Disclosure

B. Cocanougher, L. Flynn, P. Yun, M. Jain, M. Waite, R. Vasavada, and J. Wittenbach report no disclosures relevant to the manuscript. S. de Chastonay reports grant funding from Where There's a Will There's A Cure Foundation for Myotubular Myopathy during the conduct of the study. S. Chhibber, A. Innes, L. MacLaren, and T. Mozaffar report no disclosures relevant to the manuscript. A. Arai reports nonfinancial support from Siemens and nonfinancial support from Bayer outside the submitted work. S. Donkervoort,

C. Bönnemann, and A. Foley report no disclosures relevant to the manuscript. Go to Neurology.org/N for full disclosures.

Appendix Authors

Name	Location	Role	Contribution
Benjamin T. Cocanougher, BS	University of Rochester, NY; University of Cambridge, UK	Author	Major role in the acquisition of data, analyzed the data, interpreted the data, drafted the manuscript for intellectual content
Lauren Flynn, DO	NIH, Bethesda, MD	Author	Designed and conceptualized study, major role in the acquisition of data
Pomi Yun, MPH	NIH, Bethesda, MD	Author	Designed and conceptualized study, major role in the acquisition of data, analyzed the data, interpreted the data, drafted the manuscript for intellectual content
Minal Jain DSc, PT	NIH, Bethesda, MD	Author	Major role in the acquisition of data
Melissa Waite, MSPT	NIH, Bethesda, MD	Author	Major role in the acquisition of data
Ruhi Vasavada, BS	NIH, Bethesda, MD	Author	Major role in the acquisition of data
Jason D. Wittenbach, PhD	HHMI Janelia Research Campus, Ashburn, VA	Author	Analyzed the data
Sabine de Chastonay, PhD	Cure CMD, Torrance, CA	Author	Major role in the acquisition of data
Sameer Chhibber, MD	University of Calgary, Canada	Author	Major role in the acquisition of data
A. Micheil Innes, MD	Alberta Children's Hospital Research Institute, Canada	Author	Major role in the acquisition of data
Linda MacLaren, MS, CGC	Alberta Children's Hospital, Canada	Author	Major role in the acquisition of data
Tahseen Mozaffar, MD	University of California, Irvine	Author	Major role in the acquisition of data

Continued

Appendix *(continued)*

Name	Location	Role	Contribution
Andrew E. Arai, MD	NIH, Bethesda, MD	Author	Major role in the acquisition of data, analyzed the data
Sandra Donkervoort, MS, CGC	NIH, Bethesda, MD	Author	Designed and conceptualized study, major role in the acquisition of data
Carsten G. Bönnemann, MD	NIH, Bethesda, MD	Author	Designed and conceptualized study, major role in the acquisition of data, analyzed the data, interpreted the data, drafted the manuscript for intellectual content
A. Reghan Foley, MD	NIH, Bethesda, MD	Corresponding author	Designed and conceptualized study, major role in the acquisition of data, analyzed the data, interpreted the data, drafted the manuscript for intellectual content

References

1. Jungbluth H, Gautel M. Pathogenic mechanisms in centronuclear myopathies. Front Aging Neurosci 2014;6:339.
2. Heckmatt JZ, Sewry CA, Hodes D, Dubowitz V. Congenital centronuclear (myotubular) myopathy: a clinical, pathological and genetic study in eight children. Brain 1985;108:941–964.
3. Sawchak JA, Sher JH, Norman MG, Kula RW, Kula SA. Centronuclear myopathy heterogeneity: distinction of clinical types by myosin isoform patterns. Neurology 1991;41:135–140.
4. Dahl N, Hu LJ, Chery M, et al. Myotubular myopathy in a girl with a deletion at Xq27-q28 and unbalanced X inactivation assigns the MTM I gene to a 600-kb region. Am J Hum Genet 1995;56:1108.
5. Tanner SM, Ørstavik KH, Kristiansen M, et al. Skewed X-inactivation in a manifesting carrier of X-linked myotubular myopathy and in her non-manifesting carrier mother. Hum Genet 1999;104:249–253.
6. Hammans SR, Robinson DO, Moutou C, et al. A clinical and genetic study of a manifesting heterozygote with X-linked myotubular myopathy. Neuromuscul Disord 2000;10:133–137.
7. Flex E, De Luca A, D'Apice MR, et al. Rapid scanning of myotubularin (MTM1) gene by denaturing high-performance liquid chromatography (DHPLC). Neuromuscul Disord 2001;12:501–505.
8. Sutton IJ, Winer JB, Norman AN, Liechti-Gallati F, MacDonald F. Limb girdle and facial weakness in female carriers of X-linked myotubular myopathy mutations. Neurology 2001;57:900–902.
9. Schara U, Kress W, Tücke J, Mortier W. X-linked myotubular myopathy in a female infant caused by a new MTM1 gene mutation. Neurology 2003;60:1363–1365.
10. Jungbluth H, Sewry CA, Buj-Bello A, et al. Early and severe presentation of X-linked myotubular myopathy in a girl with skewed X-inactivation. Neuromuscul Disord 2003;13:55–59.
11. Grogan PM, Tanner SM, Ørstavik KH, et al. Myopathy with skeletal asymmetry and hemidiaphragm elevation is caused by myotubularin mutations. Neurology 2005;64:1638–1640.
12. Pénisson-Besnier I, Biancalana V, Reynier P, et al. Diagnosis of myotubular myopathy in the oldest known manifesting female carrier: a clinical and genetic study. Neuromuscul Disord 2007;17:180–185.
13. Drouet A, Ollagnon-Roman E, Streichenberger N, et al. Expression hemicorporelle d'une myopathie myotubulaire liee a l'X (XLMTM) chez deux des trois femmes conductrices d'une meme famille sans cas masculin. Rev Neurol 2008;164:169–176.
14. Bevilacqua JA, Bitoun M, Biancalana V, et al. "Necklace" fibers, a new histological marker of late-onset MTM1-related centronuclear myopathy. Acta Neuropathol 2009;117:283–291.
15. Hedberg C, Lindberg C, Máthé G, et al. Myopathy in a woman and her daughter associated with a novel splice site MTM1 mutation. Neuromuscul Disord 2012;22:244–251.
16. Fattori F, Maggi L, Bruno C, et al. Centronuclear myopathies: genotype-phenotype correlation and frequency of defined genetic forms in an Italian cohort. J Neurol 2015;262:1728–1740.
17. Savarese M, Musumeci O, Giugliano T, et al. Novel findings associated with MTM1 suggest a higher number of female symptomatic carriers. Neuromuscul Disord 2016;26:292–299.
18. Biancalana V, Scheidecker S, Miguet M, et al. Affected female carriers of MTM1 mutations display a wide spectrum of clinical and pathological involvement: delineating diagnostic clues. Acta Neuropathol 2017;134:889–904.
19. Bérard C, Payan C, Hodgkinson I, Fermanian J. A motor function measure scale for neuromuscular diseases. Construction and validation study. Neuromuscul Disord 2005;15:463–470.
20. Wittenbach JD, Cocanougher BT, Yun P, Foley AR, Bönnemann CG. MuscleViz: Free Open-Source Software for Muscle Weakness Visualization. J Neuromuscul Dis. 2019;6:263–266.
21. Allen RC, Zoghbi HY, Moseley AB, Rosenblatt HM, Rosenblatt JW. Methylation of HpaII and HhaI sites near the polymorphic CAG repeat in the human androgen-receptor gene correlates with X chromosome inactivation. Am J Hum Genet 1992;51:1229–1239.
22. Haller JA, Kramer SS, Lietman SA. Use of CT scans in selection of patients for pectus excavatum surgery: a preliminary report. J Pediatr Surg 1987;22:904–906.
23. Herman GE, Finegold M, Zhao W, de Gouyon B, de Gouyon A Medical complications in long-term survivors with X-linked myotubular myopathy. J Pediatr 1999;134:206–214.
24. Pierson CR, Dulin-Smith AN, Durban AN, et al. Modeling the human MTM1 p.R69C mutation in murine Mtm1 results in exon 4 skipping and a less severe myotubular myopathy phenotype. Hum Mol Genet 2012;21:811–825.
25. Herman GE, Kopacz K, Zhao W, Mills PL, Mills A, Das S. Characterization of mutations in fifty North American patients with X-linked myotubular myopathy. Hum Mutat 2002;19:114–121.
26. McEntagart M, Parsons G, Buj-Bello A, et al. Genotype-phenotype correlations in X-linked myotubular myopathy. Neuromuscul Disord 2002;12:939–946.
27. Raess MA, Friant S, Cowling BS, Laporte J. WANTED: dead or alive: myotubularins, a large disease-associated protein family. Adv Biol Regul 2017; 63:49–58.
28. Tasca G, Monforte M, Iannaccone E, et al. Upper girdle imaging in facioscapulohumeral muscular dystrophy. PLoS One 2014;9:e100292.
29. Rijken NH, van der Kooi EL, Hendriks JC, et al. Skeletal muscle imaging in facioscapulohumeral muscular dystrophy, pattern and asymmetry of individual muscle involvement. Neuromuscul Disord 2014;24:1087–1096.
30. Tasca G, Monforte M, Iannaccone E, et al. Muscle MRI in female carriers of dystrophinopathy. Eur J Neurol 2012;19:1256–1260.
31. Sarkozy A, Deschauer M, Carlier RY, et al. Muscle MRI findings in limb girdle muscular dystrophy type 2L. Neuromuscul Disord 2012;22(suppl 2):S122–S129.
32. Astrea G, Schessl J, Clement E, et al. Muscle MRI in FHL1-linked reducing body myopathy. Neuromuscul Disord 2009;19:689–691.
33. Ten Dam L, van der Kooi AJ, Rövekamp F, Linssen WH, de Visser M. Comparing clinical data and muscle imaging of DYSF and ANO5 related muscular dystrophies. Neuromuscul Disord 2014; 24:1097–1102.
34. Kristiansen M, Knudsen GP, Bathum L, et al. Twin study of genetic and aging effects on X chromosome inactivation. Eur J Hum Genet 2005;13:599–606.
35. Kristiansen M, Knudsen GP, Tanner SM, et al. X-inactivation patterns in carriers of X-linked myotubular myopathy. Neuromuscul Disord 2003;13:468–471.
36. Busque L, Paquette Y, Provost S, et al. Skewing of X-inactivation ratios in blood cells of aging women is confirmed by independent methodologies. Blood 2009;113:3472–3474.
37. Cowling BS, Chevremont T, Prokic I, et al. Reducing dynamin 2 expression rescues X-linked centronuclear myopathy. J Clin Invest 2014;124:1350–1363.
38. Tasfaout H, Buono S, Guo S, et al. Antisense oligonucleotide-mediated Dnm2 knockdown prevents and reverts myotubular myopathy in mice. Nat Comm 2017;8:15661.
39. Royer B, Hnia K, Gavriilidis C, Tronchère H, Tosch V, Laporte J. The myotubularin-amphiphysin 2 complex in membrane tubulation and centronuclear myopathies. EMBO Rep 2013;14:907–915.
40. Anderson CL, Brown CJ. Variability of X chromosome inactivation: effect on levels of TIMP1 RNA and role of DNA methylation. Hum Genet 2002;110:271–278.
41. Carrel L, Willard HF. X-inactivation profile reveals extensive variability in X-linked gene expression in females. Nature 2005;434:400–404.
42. Cotton AM, Ge B, Light N, Adoue V, Pastinen T, Brown CJ. Analysis of expressed SNPs identifies variable extents of expression from the human inactive X chromosome. Genome Biol 2013;14:R122.
43. Berletch JB, Ma W, Yang F, Shendure WS, Noble WS, Disteche CM, Deng X. Escape from X inactivation varies in mouse tissues. PLoS Genet 2015;11:e1005079.
44. Gurgel-Giannetti J, Zanoteli E, de Castro Concentino EL, et al. Necklace fibers as histopathological marker in a patient with severe form of X-linked myotubular myopathy. Neuromuscul Disord 2012;22:541–545.